

55-20

393878

358067

1997

NASA/ASEE SUMMER FACULTY FELLOWSHIP PROGRAM

MARSHALL SPACE FLIGHT CENTER
UNIVERSITY OF ALABAMA
IN HUNTSVILLE

ROCKET PROPELLANT DUCTS :
(cryogenic fuel lines)
FIRST CUT APPROXIMATIONS AND DESIGN GUIDANCE

Prepared by: William V. Brewer, Ph.D.

Academic Rank: Professor

Institution and Department: Jackson State University
School of Science & Technology
Technology

NASA/MSFC:

Office: Propulsion Laboratory
Division: Propulsion and Mechanical Systems
Branch: Mechanical Systems Design

MSFC Colleagues: Lance Moore
Tim Ezell

1

2

3

INTRODUCTION

Problem: The design team has to set parameters before analysis can take place. Analysis is customarily a thorough and time consuming process which can take weeks or even months. Only when analysis is complete can the designer obtain feedback. If margins are negative, the process must be repeated to a greater or lesser degree until satisfactory results are achieved. Reduction of the number of iterations thru this loop would beneficially conserve time and resources.

Task: Develop relatively simple, easy to use, guidelines and analytic tools that allow the designer to evaluate what effect various alternatives may have on performance as the design progresses. Easy to use is taken to mean closed form approximations and the use of graphic methods. Simple implies that 2-d and quasi 3-d approximations be exploited to whatever degree is useful before more resource intensive methods are applied. The objective is to avoid the grosser violation of performance margins at the outset.

Initial efforts are focused on thermal expansion/contraction and rigid body kinematics as they relate to propellant duct displacements in the gimbal plane loop (GPL). Purpose of the loop is to place two flexible joints on the same two orthogonal intersecting axes as those of the rocket motor gimbals. This supposes the ducting will flex predictably with independent rotations corresponding to those of the motor gimbal actions. It can be shown that if GPL joint axes do not coincide with motor gimbal axes, displacement incompatibilities result in less predictable movement of the ducts.

OBSERVATION

Pierced Ear Principle: Violation of this principle guarantees that for combined rotations of the motor about both gimbal axes, joint and gimbal axes will not coincide thus defeating the purpose of the GPL. This principle has been used in the past [1] but is not generally recognized in the design community. The principle may be stated as follows:

The axis of the GPL joint attached to the motor must be coincident with the axis piercing the ears of the gimbal conjugate that attaches to the motor.

The axis of the GPL joint closest to the vehicle must be coincident with the axis piercing the ears of the gimbal conjugate that attaches to the vehicle.

In the absence of compelling reasons to the contrary this principle is a reasonable candidate for a design guideline (or rule of thumb).

That GPL performance does not always conform to expectations has been noted by practitioners with the result that a third joint in a line perpendicular to the gimbal plane is usually included to allow for thermal expansion and manufacturing imprecision. If the "as-built" GPL configuration succeeds in achieving coincident joint and gimbal axes, this will not be the case over the entire operating temperature range. Rocket motors experience temperatures in negative hundreds of degrees F. in their cryogenic propellant conduits contrasting with combustion chamber temperatures in thousands of degrees F.

APPROXIMATION MODELS

Sample calculations and coordinate system used in the following discussion are for the PT AI 60K Engine [2]. The x-y plane passes thru the gimbal axes and is the plane intended for the GPL.

To explore thermal effects on the GPL configuration, the 3 joints mentioned above are examined 2 at a time in planes parallel to the 3 coordinate planes (Figure 1). This was done graphically with the assistance of an AutoCad package. Results thus achieved are superposed as a measure of dimensional incompatibility that must be resolved by the 3-d, 3 joint space linkage. MathCad software was used for this purpose and gimbal rotations were included in addition to the thermal expansion estimate. Results of sample calculations (Figure 2) are superposed for the extreme articulations of the motor gimbals (± 5 degrees). Where estimates in 2 planes are based on thermal expansion of the same pipe lengths the results are averaged; where based on different lengths they are simply added. Results for this example indicated that thermal expansion has a relatively greater impact than does gimbal rotation thru a small angle. Thermal effects were, in this case, based on gross aggregations of temperature distribution. Larger rotations can be explored using the model. Extent and source of problems may be estimated on a comparative basis with experience of the user.

A 4th 2-d plane passing thru the three joints may also be of value (Figure 3). Assume 3 ball joints where the terminal joints #1 and #3 have a conjugate attached respectively: joint #1 to the motor; and joint #3 to the vehicle frame. Then the locations of these joints are known. The other conjugates of Joints #1 and #3 are attached to the 2 links which span the distance between them. The links are connected by the middle joint, #2. If the middle joint were broken then the free end of each link could move on a spherical surface the radius of which is the length of the link. The circle representing the intersection of the 2 spheres is the domain of possible locations of the middle joint. The circle also may be visualized as the intersection of 2 cones whose elements are the length of the links. A plane passed thru the 3 joints sees the intersecting cones as triangles. As thermal expansion and/or gimbal rotation changes, the center locations and radii of the spheres change with a corresponding change in the triangular intersections. Comparing these changes with the as-built images gives a measure of the accommodation necessary from the linkage in 3-d.

RESULTS

In the example where these methods were applied to the PT AI 60K engine GPL, results indicate relatively small perturbations coming from the ± 5 degree gimbal rotations compared with those caused by thermal expansion.

CONCLUSIONS

Where as in the example thermal effects dominated the results, other designs in which larger gimbal rotations are used may produce a significantly different result which may be quantified with the methods outlined here.

Thermal effects amplify distortions caused by gimbal rotation by moving joints in the Gimbal Plane Loop away from the gimbal plane.

Pierce Ear Principle is generally a very inexpensive precaution that should be observed by the design community in practice, absent any compelling need to the contrary.

ACKNOWLEDGEMENTS

I would like to thank my mentors for all the assistance rendered, especially in providing appropriate background literature and making comfortable and convenient work space available with all the required utilities.

REFERENCES

- [1] **Liquid Rocket Lines, Bellows, Flexible Hoses, and Filters**, NASA Space Vehicle Design Criteria (Chemical Propulsion), NASA SP-8123, April 1977, p.83, Figure 41.
- [2] "PT AI 60K Engine Interface Control Drawing", No. 96M30760, Code 14981, MSFC/NASA Huntsville AL, 6/97.

Gimbal Plane Loop Kinematic Displacement Incompatibility
Caused by Thermal Expansion

page 6

GP-2D-3P

SUMMARY OF RESULTS

Approximation by 2-D
Superposition

LOx Feed Line

COMBINATIONS of THERMAL EXPANSIONS and EXTREME GIMBAL ROTATIONS in 3 COORDINATE PLANES

NOTE : Multiple estimates of a quantity based on a thermal expansion of the same length of pipe are averaged.
Multiple estimates of a quantity based on a thermal expansion of different lengths of pipe are added.

NOTE : 1st index identifies x - rotation ; 2nd index identifies y - rotation.
+ indicated by 1 ; - indicated by 2 .

positive x-rotation positive y-rotation	positive x-rotation negative y-rotation	negative x-rotation positive y-rotation	negative x-rotation negative y-rotation
$\Delta X_{a_{11}} = 0.363$	$\Delta X_{a_{12}} = 0.363$	$\Delta X_{a_{21}} = 0.517$	$\Delta X_{a_{22}} = 0.517$
$\Delta Y_{a_{11}} = 0.412$	$\Delta Y_{a_{12}} = 0.441$	$\Delta Y_{a_{21}} = 0.453$	$\Delta Y_{a_{22}} = 0.482$
$\Delta Z_{a_{11}} = 0.097$	$\Delta Z_{a_{12}} = 0.111$	$\Delta Z_{a_{21}} = 0.108$	$\Delta Z_{a_{22}} = 0.122$
Vector Sum of Displacement Incompatibilities :			
$\Delta R_{a_{11}} = 0.558$	$\Delta R_{a_{12}} = 0.582$	$\Delta R_{a_{21}} = 0.696$	$\Delta R_{a_{22}} = 0.718$

Figure 2: Example Results for 2-D Approximations of Dimensional Incompatibility

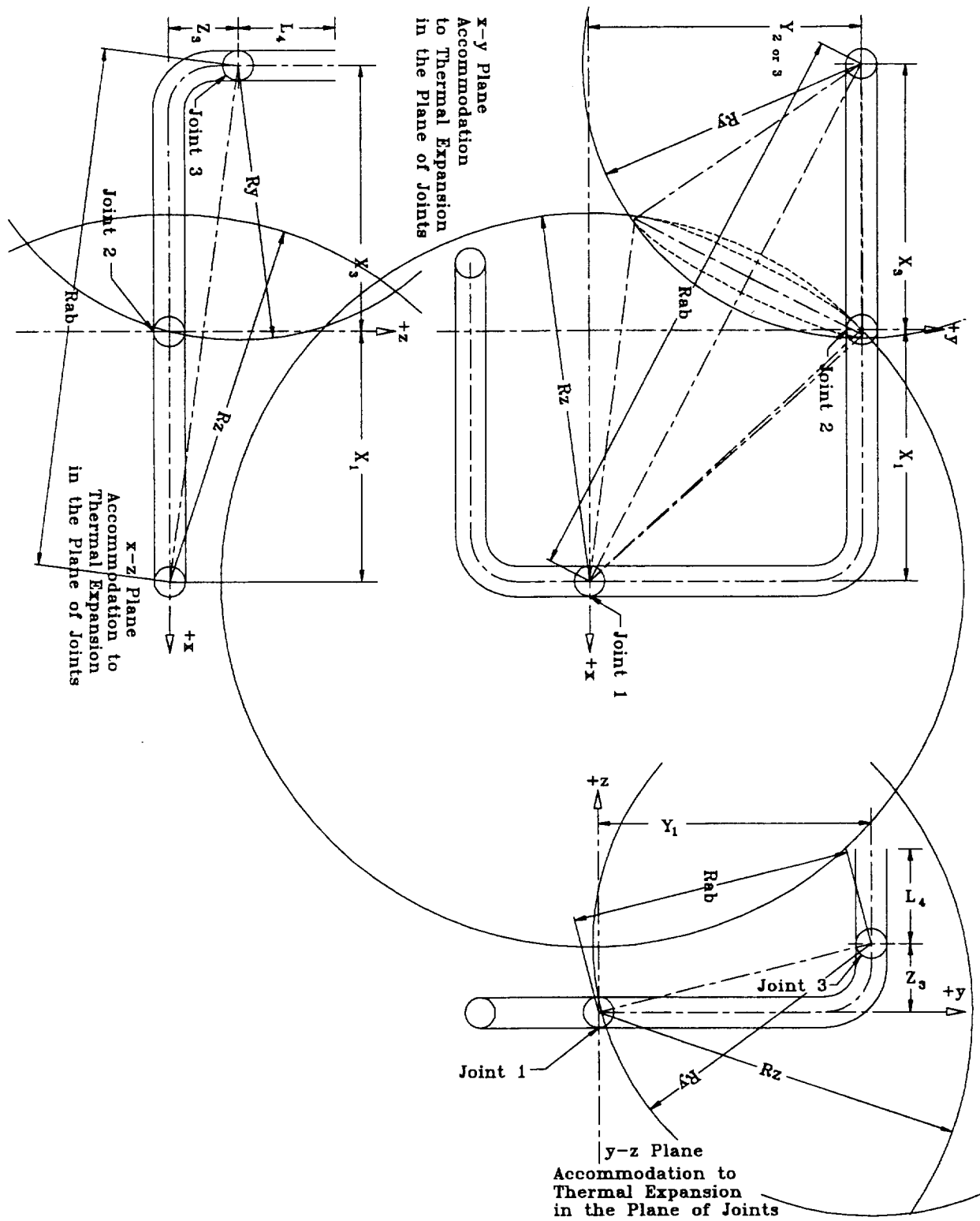


Figure 3:
Accommodation to Thermal Expansion in the Plane of Joints

